ADNI Data Analysis

Aaron Shikh

1 Introduction

Alzheimer's Disease is a progressive neurodegenerative disorder characterized by measurable changes in brain structure over time. A region of particular interest is the corpus callosum, a large bundle of nerve fibers that connects the two hemispheres of the brain, which has been shown to exhibit significant structural differences between healthy individuals and those with Alzheimer's. Shape-based analysis of the corpus callosum can therefore provide valuable insights into the diagnosis and progression of the disease.

However, traditional approaches to statistical analysis of shape data often treat brain structures as vectors in the Euclidean space. These non-manifold methods fail to account for the fact that shapes lie on nonlinear spaces, leading to distortions in distance, averaging, and hypothesis testing. For example, averaging shapes directly in Euclidean space may yield an anatomically implausible structure due to the influence of variations such as rotation, translation, or scale.

To address these limitations, we turn to shape spaces, which allow for statistical analysis of shapes. In this paper, we analyze corpus callosum shapes from the Alzheimer's Disease Neuroimaging Initiative (ADNI) dataset in the setting of Kendall's shape space. Each shape is represented by 50 anatomical landmarks in $\mathbb{R}^2$. We compute Frechet means, visualize shape variability, and statistically compare populations using two-sample hypothesis tests.

The rest of the paper is structured as follows. In Section 2, we introduce the mathematical background of Kendall's shape space and the formulas used for shape analysis. Section 3 presents results on simulated shape data to validate the methods under ideal conditions. Section 4 applies the same analysis to the ADNI dataset, where we examine group differences in corpus callosum shape and evaluate their statistical significance.

2 Preliminaries

This section introduces the mathematical foundation necessary to analyze shapes on nonlinear spaces, Kendall's shape space in this case.

A **smooth manifold** M is a topological space that locally resembles Euclidean space and allows for smooth differentiation [1]. At any point $p \in M$, the **tangent space** T_pM is defined as the span of velocity vectors of all smooth curves passing through p. If M is equipped with a smoothly varying inner product $g_p(\cdot, \cdot)$ on T_pM, it becomes a **Riemannian manifold** (M, g).

In such spaces, the shortest path between two points $p, q \in M$ is called a **geodesic**. The **exponential map** $\exp_p : T_pM \to M$ moves from p in the direction of a tangent vector $v \in T_pM$ for unit time along a geodesic. Its inverse, the **logarithm map** $\log_p : M \to T_pM$, maps a point q on the manifold back to the tangent vector v such that $\exp_p(v) = q$.

2.1 Shape as a Quotient Space

Let a shape be represented by a configuration of k landmarks in $\mathbb{R}^n$, stored as a matrix $X \in \mathbb{R}^{k \times n}$. To analyze shape independently of translation, scaling, and rotation, we construct a shape space by removing these effects using quotient spaces.

38th Conference on Neural Information Processing Systems (NeurIPS 2024).

Translation. To remove translation, we center each shape by subtracting the centroid from all landmarks. This projects X onto the subspace of centered configurations:

$$\mathcal{C}_{k,n} = \left\{ X \in \mathbb{R}^{k \times n} \,\middle|\, \sum_{i=1}^{k} X_{i,\cdot} = 0 \right\}.$$

Scaling. To remove scale, we normalize each centered shape to lie on the unit sphere under the Frobenius norm:

$$S = \{ X \in \mathcal{C}_{k,n} \mid \|X\|_F = 1 \}.$$

Rotation. Finally, we remove the effect of rotation by considering shapes equivalent if one can be obtained from the other through a rotation in $\mathrm{SO}(n)$, the group of special orthogonal n×n matrices. So two centered and scaled configurations X and Y represent the same shape if there exists a rotation matrix $O^* \in \mathrm{SO}(n)$ such that:

$$Y = XO^*.$$

2.2 Kendall's Shape Space

Kendall's shape space combines all of the previous quotient spaces and compares shapes defined by k ordered landmarks in $\mathbb{R}^n$ while removing irrelevant variation from translation, rotation, and scaling [3]. Let $L_{n,k}$ be the space of all $k \times n$ matrices of landmarks. The similarity group $G = \mathrm{SO}(n) \times \mathbb{R}^+ \times \mathbb{R}^n$ acts on $L_{n,k}$ by rotation, scaling, and translation respectively. The shape space is then the quotient space:

$$\Sigma_k^n = L_{n,k}/G.$$

To compute in this space, each shape is centered (translation removed), scaled to unit Frobenius norm (scale removed), and optimally rotated (using Procrustes alignment) to minimize the Frobenius distance. The geodesic distance between two such shapes is given by:

$$d(X_1, X_2) = \arccos\left(\mathrm{tr}(X_1^\top X_2 O^*)\right),$$

where O^* is the optimal rotation aligning X_2 to X_1.

2.3 Fréchet Mean

The Frechet mean is a generalization of the Euclidean mean to non-Euclidean spaces, like Kendall's shape space. Given a set of shapes $\{X_1, X_2, \ldots, X_n\}$ that lie on a Riemannian manifold $\mathcal{M}$, the Frechet mean $\hat{\mu}$ is defined as the point that minimizes the sum of squared geodesic distances to all sample shapes:

$$\hat{\mu} = \arg\min_{p \in \mathcal{M}} \sum_{i=1}^{n} d^2(p, X_i)$$

Where the distance $d(\cdot, \cdot)$ is the spherical Procrustes distance, which accounts for translation, scaling, and optimal rotation between centered, normalized shapes.

2.4 Energy Distance and Permutation Test

The energy distance is a metric for comparing distributions based on pairwise distances between samples [4]. Given two shape samples $X = \{x_1, \ldots, x_n\}$ and $Y = \{y_1, \ldots, y_m\}$, the energy statistic is:

$$\hat{D}_{ts} = \frac{2}{nm} \sum_{i=1}^{n} \sum_{j=1}^{m} d(x_i, y_j) - \frac{1}{n^2} \sum_{i,j=1}^{n} d(x_i, x_j) - \frac{1}{m^2} \sum_{i,j=1}^{m} d(y_i, y_j).$$

To test whether two samples come from the same distribution, we perform a permutation test [2]: repeatedly shuffle group labels, recompute $\hat{D}_{ts}$, and compare the observed statistic to the null distribution, getting a final p-value which can be used to interpret significance.

3 Simulation Results

Before analyzing real brain data, we apply our shape analysis techniques to a simulated dataset consisting of three distinct shape categories: hands, hammers, and glasses. This serves as a proof-of-concept, allowing us to evaluate the behavior of Fréchet means, permutation testing, and clustering under ideal conditions where the group structure is known and separated. The results here show that the shape analysis we use is capable of detecting differences when they exist in shape groups.

3.1 Fréchet Means of Shape Groups

We first compute and visualize the Fréchet means of the three simulated shape classes. As shown in Figure 1, the mean shapes for glasses, hammers, and hands are easily distinguishable. Each shape maintains its structural shape, which is expected given the well separated nature of the shape dataset. This shows that given more complex and less separated data, we may be able to see some more subtle and important differences in groups.

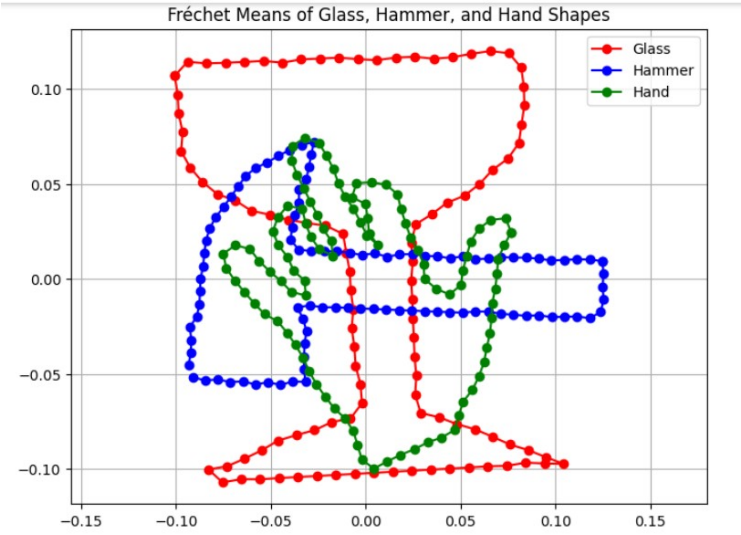

Figure 1: Fréchet means for Glass, Hammer, and Hand shapes.

3.2 Two-Sample Permutation Test and Distance Matrix

We next test for statistical differences between shape groups using the energy distance and permutation testing, just as we later do with the ADNI dataset. In this case, the Kendall shape distance matrix in Figure 2 shows the classic block structure: low within-group distances and high between-group distances, forming a clear checkerboard pattern.

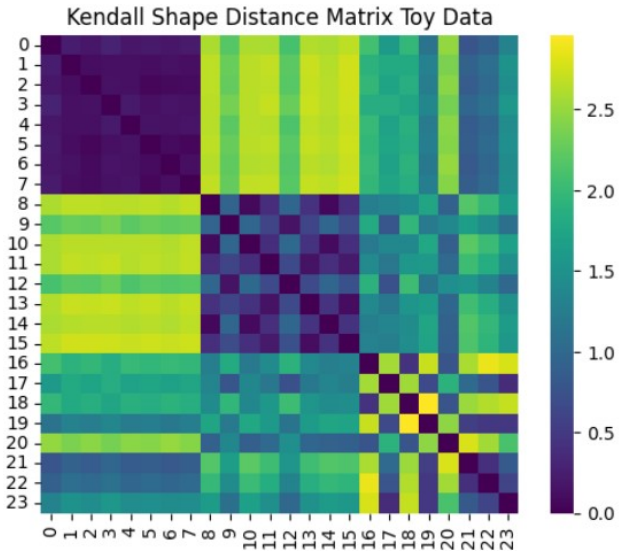

Figure 2: Kendall shape distance matrix for simulation data

The results of the permutation tests, shown in Figure 3, confirm this separation: all pairwise comparisons between groups are statistically significant with p-values close to zero. These results are expected in this simulated setting and show that the energy distance approach can detect known shape differences.

Comparison	Energy Statistic	Permutation p-value	Significant
Glass vs Hammer	4.534990	0.00000	Yes
Glass vs Hand	1.553576	0.00003	Yes
Hammer vs Hand	1.101210	0.00989	Yes

Figure 3: Permutation test results for all toy shape comparisons.

3.3 Clustering Analysis

Finally, we apply hierarchical clustering to see if we can again show the three original shape categories in an unsupervised way, just using the Kendall Shape Space distance matrix. The dendrogram in Figure 4 is cut at three clusters, which matches the number of shape groups, and the labels correspond perfectly.

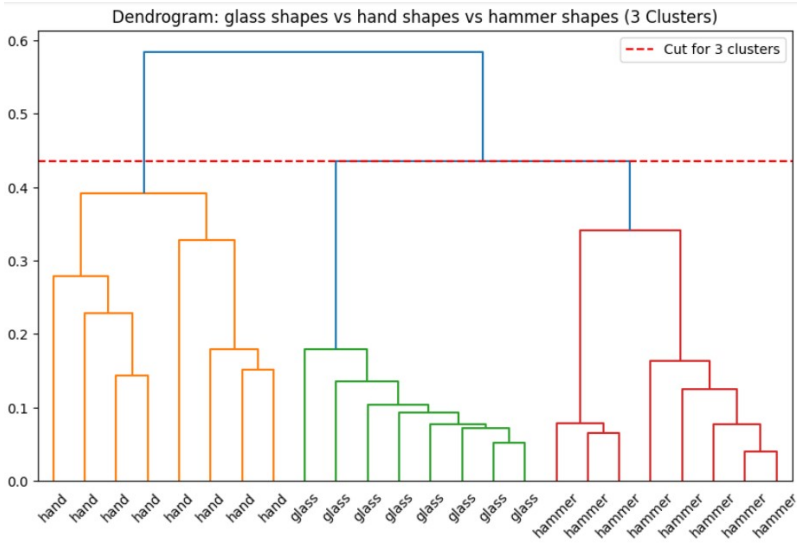

Figure 4: Dendrogram for toy dataset cut into three clusters

The resulting cluster distribution (Figure 5) shows perfect matching: each original shape group maps exactly to one cluster, demonstrating that the Kendall distances contain enough structure for accurate classification in an ideal dataset.

Cluster	1	2	3
Shape			
glass	0	8	0
hammer	0	0	8
hand	8	0	0

Figure 5: Cluster assignments for the simulation dataset

Overall, the simulation data analysis confirms that our methods are capable of detecting and separating meaningful shape differences. This establishes the main idea for applying the same tools to the ADNI data, where the task is far more challenging due to lots of biological variability and inconsistency in human brain measurements.

4 Experimental Results

In this section, we move on from the simulation data to analyze the corpus callosum shape data from the ADNI dataset. We divide subjects into three pairs of comparison groups: Male Control vs. Male Alzheimer's, Female Control vs. Female Alzheimer's, and Combined Control vs. Combined Alzheimer's. Each shape is represented by 50 landmarks in $\mathbb{R}^2$ and is analyzed in Kendall's shape space. For each comparison, we compute Fréchet means, conduct two sample permutation hypothesis tests based on the energy distance, and perform hierarchical clustering.

4.1 Fréchet Means of Shape Groups

We begin by plotting the Fréchet means of all groups in a single figure to compare the shape variation, and start to make hypothesis about which groups we think may have some significant differences.

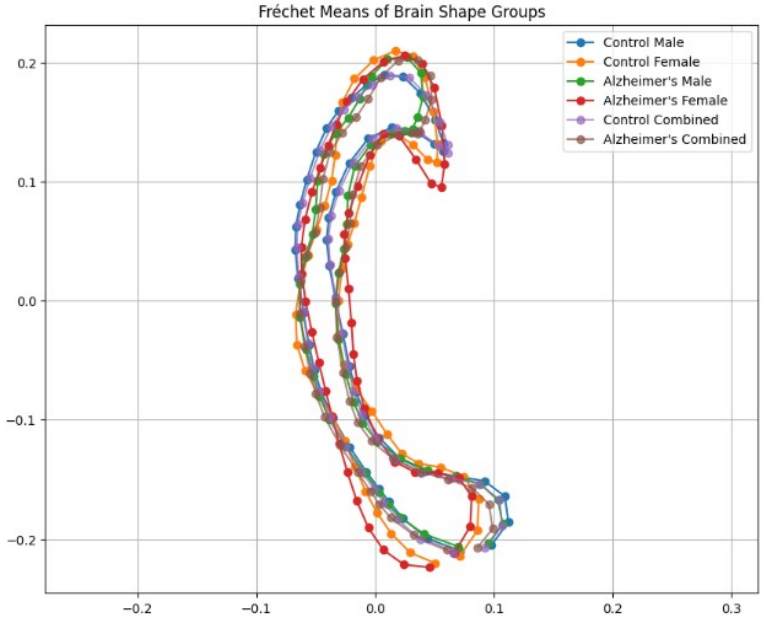

Figure 6: Fréchet mean shapes for all ADNI subgroups

Figure 6 shows an overlay of Fréchet means for all six subgroups. The most noticeable differences appear in the top and bottom regions of the corpus callosum. Across groups, control subjects consistently show a more elongated and curved shape, particularly with a sharper top arch and more pronounced curvature at the bottom tip. However, Alzheimer's groups tend to have rounder top and bottom sections, suggesting compression or atrophy.

To further explore these differences in detail, we plotted groupwise comparisons in Appendix A.1 (Figures 10, 11, and 12).

The female comparison (Figure 11) shows that the control shape retains a distinctly pointed and arched top, while the Alzheimer's mean shape appears slightly more elongated vertically and somewhat smoother in curvature. In contrast, the male comparison (Figure 10) reveals more consistent vertical length between groups, but the Alzheimer's shape displays a noticeably smoother top region and reduced curvature throughout. The control shape is slightly larger particularly in the top arc.

The combined group comparison (Figure 12) averages out within-sex variability. The control shape had a more pronounced curve at the top and a sharper bend. The Alzheimer's group, shows a smoother, more rounded top and appears slightly compressed near the top region. While the overall shape difference is small, these patterns still suggest that Alzheimer's disease is associated with potentially significant geometric deformation, which we will explore in greater detail in the next section.

4.2 Two-Sample Permutation Test and Distance Matrices

After analyzing Fréchet mean shapes for each group, we assess the statistical significance of shape differences using the energy distance. The test uses pairwise Kendall shape distances to evaluate whether two samples are likely drawn from the same distribution.

In theory, when visualizing the full pairwise distance matrix between two distinct groups, we expect to observe a 2×2 block (or checkerboard) structure: low distances within each group (top-left and bottom-right blocks), and high distances between groups (top-right and bottom-left). However, as shown in Appendix A.2 (Figures 13, 14, and 15), this checkerboard pattern is not immediately

obvious in the distance matrices. The reason is that the Kendall shape distances are quite small, and the variation between and within groups is small. As a result, visual inspection of the matrices is insufficient for drawing conclusions, which requires formal hypothesis testing via two sample permutation tests.

Comparison	Energy Statistic	Permutation p-value	Significant
Male Control vs. Male Alzheimer's	0.004301	0.007	Yes
Female Control vs. Female Alzheimer's	0.003457	0.027	Yes
Combined Control vs. Combined Alzheimer's	0.003298	0.000	Yes

Figure 7: Permutation test results comparing shape distributions

As shown in Figure 7, all three group comparisons have statistically significant differences in shape distributions. This confirms the patterns observed in the Fréchet mean analysis, where Alzheimer's groups consistently showed smoother, more compressed corpus callosum shapes compared to controls. The visual and statistical results together support our hypothesis that Alzheimer's disease leads to geometric changes in brain structure. These changes are detectable across sexes and preserved when groups are aggregated. These findings show us the need for shape analysis for detecting small but significant geometric differences associated with the corpus callosum shapes.

4.3 Clustering Analysis

Following the hypothesis testing results, which we confirmed showed statistically significant differences between shape distributions, we now explore whether these differences are shown as meaningful group structure in the data. Using the same Kendall distance matrices, we can apply agglomerative hierarchical clustering to try to separate control and Alzheimer's shapes based on shape distance alone. However, since the distance matrices showed weak block structure and little variation overall, we do not necessarily expect perfectly separated clusters. This part is more of an exploratory step to see whether there's any group structure left in the shape distances that the hypothesis tests didn't fully capture. We also try cutting the dendrograms into more clusters than the number of original testing groups, in case finer differences show up that aren't obvious from just comparing two populations.

We first look at the combined group comparison, which includes all male and female control and Alzheimer's subjects. The dendrogram in Figure 8 is cut into eight clusters. Although this is a relatively high number, it allows us to potentially be able to detect whether control and Alzheimer's shapes tend to group together in more subtle ways.

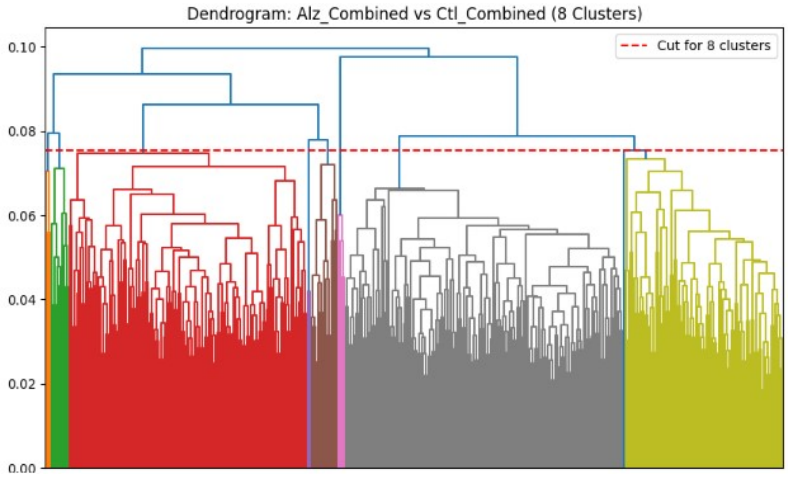

Figure 8: Dendrogram: Combined Alzheimer's vs. Combined Control (8 clusters).

The cluster distribution table (Figure 9) shows that most clusters have a very similar group membership between Alzheimer's and control subjects, meaning there is a lot of overlap in the shape space. However, Cluster 3 stands is different, with 54 Alzheimer's subjects and 78 controls: a clear imbalance that may reflect shape variation where control and Alzheimer's trajectories are different. This small separation, though not prevalent across all clusters, points to the possibility of disease specific structure in certain parts of the corpus callosum shape distribution.

Cluster	1	2	3	4	5	6	7	8
Group								
Alz_Combined	1	3	54	0	4	0	78	46
Ctl_Combined	2	7	78	2	11	4	76	43

Figure 9: Cluster distribution table for Combined Alzheimer's vs. Combined Control

We also performed similar clustering analysis on the male and female subgroups separately, using 6 and 4 clusters respectively. The dendrograms and corresponding cluster tables are included in Appendix A.3 (Figures 16, 18, 17, and 19). The female results show some structure with Cluster 3 capturing a majority of Alzheimer's subject while the male results reveal more diffuse patterns. While some limited separation exists, most clusters remain mixed, especially in the male subgroup. The female group, although not cleanly separated, shows slightly more imbalance in specific clusters, suggesting that any group structure in the data is very small and only partially observable from shape distances alone.

5 Conclusion

In this paper, we used tools from Kendall's shape space to analyze geometric differences in brain structure between control and Alzheimer's subjects. We started by validating our data pipeline on simulated shape data, where differences were large and easily detectable. This helped confirm that Fréchet means, permutation tests, and clustering work as expected under ideal conditions. We then applied the same methods to real corpus callosum shapes from the ADNI dataset. While the differences were much smaller, and the groups in the distance matrices were not very well defined, we still found consistent patterns: Alzheimer's shapes tended to be more rounded and compressed, especially in the top arcs. These differences were statistically significant in all three group comparisons, and some weak structure also appeared in the clustering results.

Compared to Euclidean approaches that ignore rotation, translation, and scaling, Kendall's shape space allowed us to find meaningful shape variation. This gave us more interpretable averages, distances, and comparisons. Going forwards, it would be interesting to combine these shape-based to longitudinal data on human brains throughout the different stages of Alzheimer's. We could fit regression models that capture how individual shapes change over time and model shapes directly in Kendall's shape space. Overall, this kind of shape analysis helps a lot with potential future work understanding how brain structure changes with disease.

A Supplementary Figures

A.1 Fréchet Mean Comparison Figures

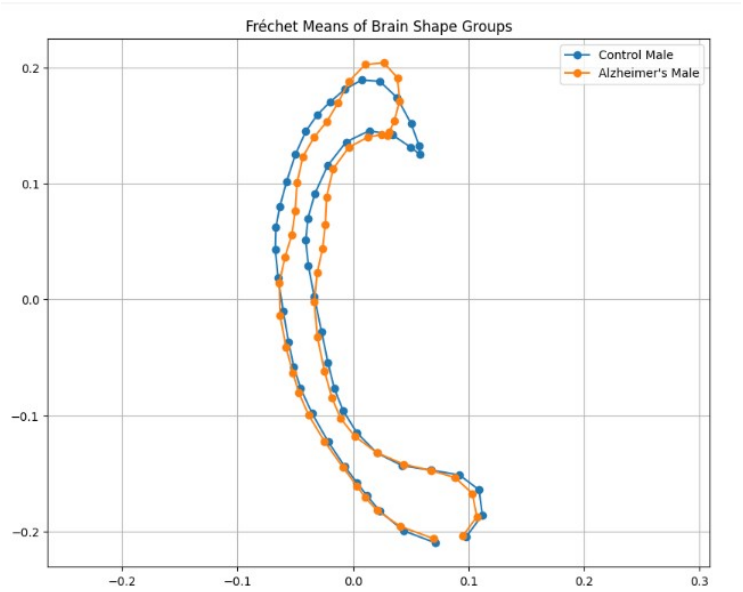

Figure 10: Fréchet means for Male Control and Male Alzheimer's

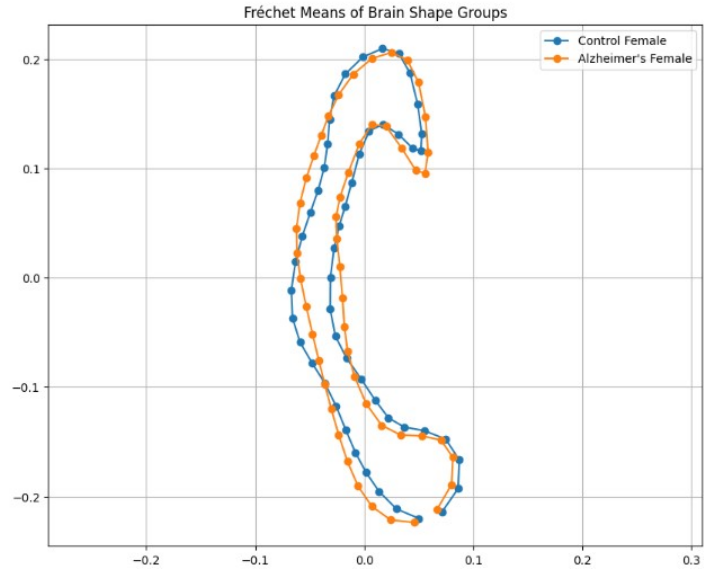

Figure 11: Fréchet means for Female Control and Female Alzheimer's

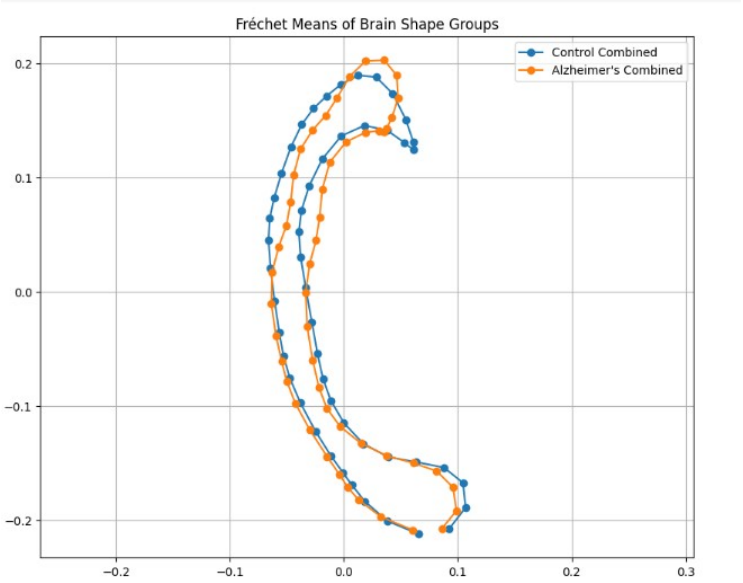

Figure 12: Fréchet means for Combined Control and Combined Alzheimer's

A.2 Distance Matrices Used for Testing

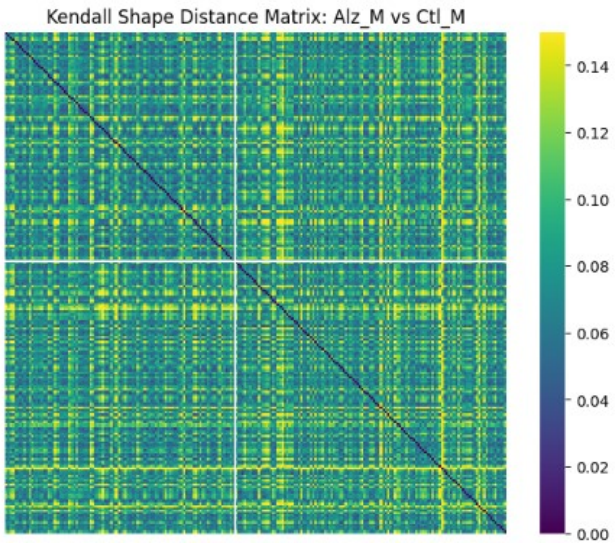

Figure 13: Kendall shape distance matrix: Male Alzheimer's vs. Male Control.

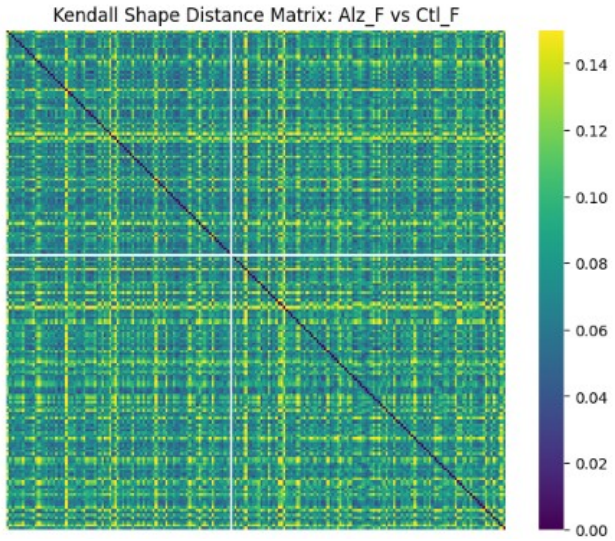

Figure 14: Kendall shape distance matrix: Female Alzheimer's vs. Female Control.

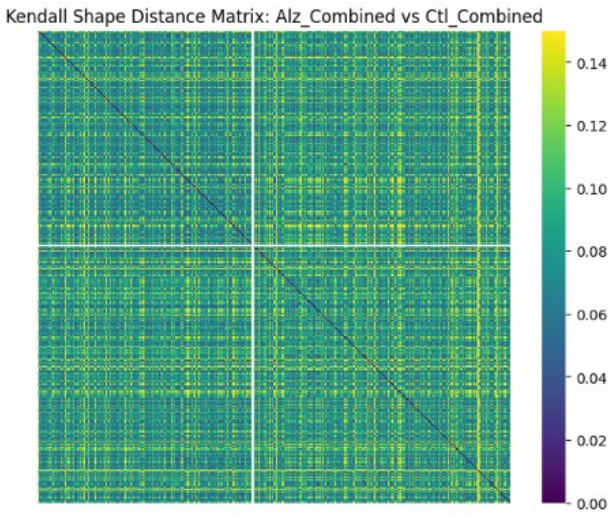

Figure 15: Kendall shape distance matrix: Combined Alzheimer's vs. Combined Control.

A.3 Additional Clustering Results

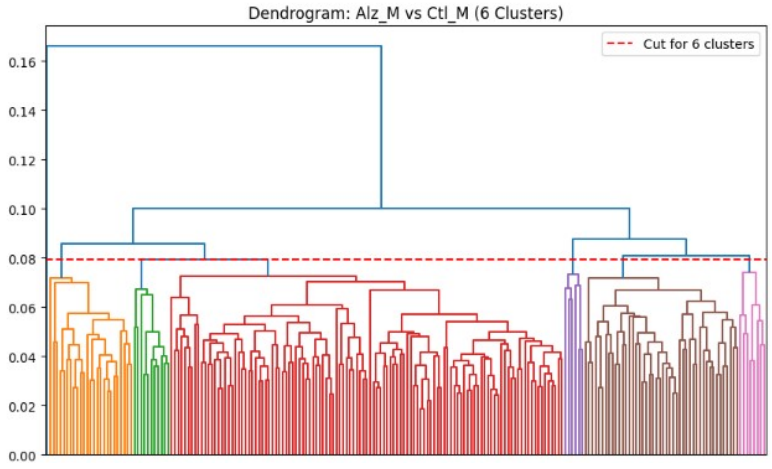

Figure 16: Dendrogram: Male Alzheimer's vs. Male Control (6 clusters).

Cluster	1	2	3	4	5	6
Group						
Alz_M	11	68	1	16	2	0
Ctl_M	14	60	5	30	6	1

Figure 17: Cluster distribution table for Male Alzheimer's vs. Male Control.

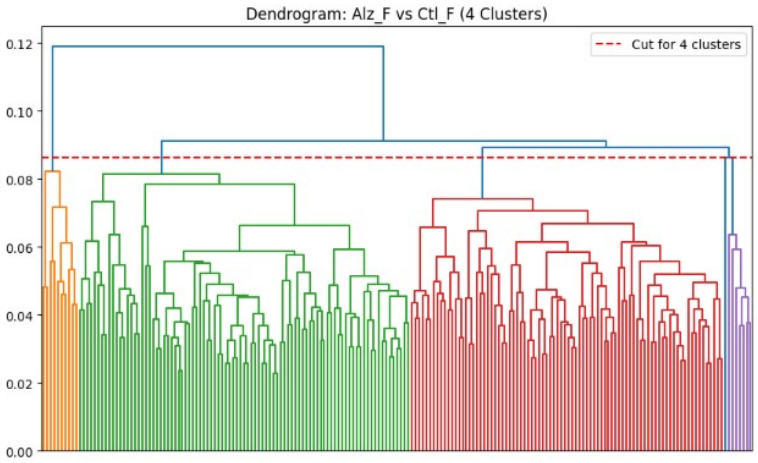

Figure 18: Dendrogram: Female Alzheimer's vs. Female Control (4 clusters).

Cluster	1	2	3	4
Group				
Alz_F	3	45	39	1
Ctl_F	7	46	47	7

Figure 19: Cluster distribution table for Female Alzheimer's vs. Female Control.

References

[1] Manfredo P. do Carmo. *Riemannian Geometry*. Birkhäuser, 1992.

[2] Phillip I. Good. *Permutation Tests: A Practical Guide to Resampling Methods for Testing Hypotheses*. Springer Series in Statistics, 2000.

[3] David G. Kendall. Shape manifolds, procrustean metrics, and complex projective spaces. *Bulletin of the London Mathematical Society*, 16(2):81–121, 1984.

[4] Maria L. Rizzo and Gábor J. Székely. Energy distance. *Wiley Interdisciplinary Reviews: Computational Statistics*, 8(1):27–38, 2016.